Full Title: Novel chP3R99 mAb reduces subendothelial retention of atherogenic lipoproteins in Insulin-Resistant rats: ***Acute treatment versus long-term protection as an idiotypic vaccine for atherosclerosis***

Running Title: Atheroprotective mAb in insulin-resistant rats

Authors: Yosdel Soto[1,2*], Arletty Hernández[1], Roger Sarduy[1], Victor Brito[1], Sylvie Marleau[3], Donna F. Vine[2], Ana M. Vázquez[3]and Spencer D. Proctor[2*]

Affiliations:

[1] Department of Immunobiology, Direction of Immunology and Immunotherapy, Centre for Molecular Immunology, Havana, Cuba.

[2] Metabolic and Cardiovascular Disease Laboratory, Group on Molecular and Cell Biology of Lipids, Alberta Diabetes and Mazankowski Heart Institutes, University of Alberta, Edmonton, AB, Canada.

[3] Faculté de Pharmacie, Université de Montréal, Montréal, QC, Canada

[4] Innovation and Managing Direction, Center for Molecular Immunology, Havana, Cuba

***Joint Corresponding Authors:**

Dr. Spencer D. Proctor, 4-002J Li Ka Shing Centre, University of Alberta, Edmonton, Alberta, Canada. T6G2P5.
Email address: spencer.proctor@ualberta.ca. ORCID ID: 0002-7597-5262

Dr. Yosdel Soto. Centre for Molecular Immunology, 216 St and 15th Ave, Atabey, Playa PO Box 16040, Havana 11600, Havana, Cuba.
Email address: yosdel@cim.sld.cu. ORCID ID: 0000-0003-1717-2514

Word Count: 9,046

ABSTRACT

Background: Atherosclerosis is triggered by the retention of apolipoprotein B-containing lipoproteins by proteoglycans. In addition to LDL, remnant lipoproteins have emerged as pivotal contributors to this pathology, particularly in the context of insulin resistance and diabetes. We have recently reported anti-atherogenic properties of a novel monoclonal antibody (chP3R99) that recognizes sulfated glycosaminoglycans on arterial proteoglycans.

Methods and Results: Solid-phase assays demonstrated that chP3R99 effectively blocked over 50% lipoprotein binding to chondroitin sulfate and vascular extracellular matrix *in vitro*. The pre-perfusion of chP3R99 (passive/competitive effect) resulted in specific antibody-arterial accumulation and reduced fluorescent lipoprotein retention by ~60% in insulin resistant JCR:LA-*cp* rats. This (passive) reduction was dose-dependent (25 µg/mL–250 µg/mL), effectively decreasing deposition of cholesterol associated with lipoproteins. In a five-week vaccination study in insulin resistant rats with (200 µg SC, once a week), chP3R99 reduced arterial lipoprotein retention, and was associated with the production of anti-CS antibodies (Ab3) able to accumulate in the arteries (dot-blot). Neither the intravenous inoculation of chP3R99 (4.5 mg/kg), nor the immunization with this antibody displayed adverse effects on lipid or glucose metabolism, insulin resistance, liver function, blood cell indices, or inflammation pathways in JCR:LA-*cp* rats.

Conclusion: Both acute (passive) and long-term administration of chP3R99 antibody reduced LDL and remnant lipoprotein interaction with proteoglycans in an insulin-resistant setting. These findings support the innovative approach of targeting pro-atherogenic lipoprotein retention by this mAb as a passive therapy or as an idiotypic vaccine for atherosclerosis.

GRAPHICAL ABSTRACT

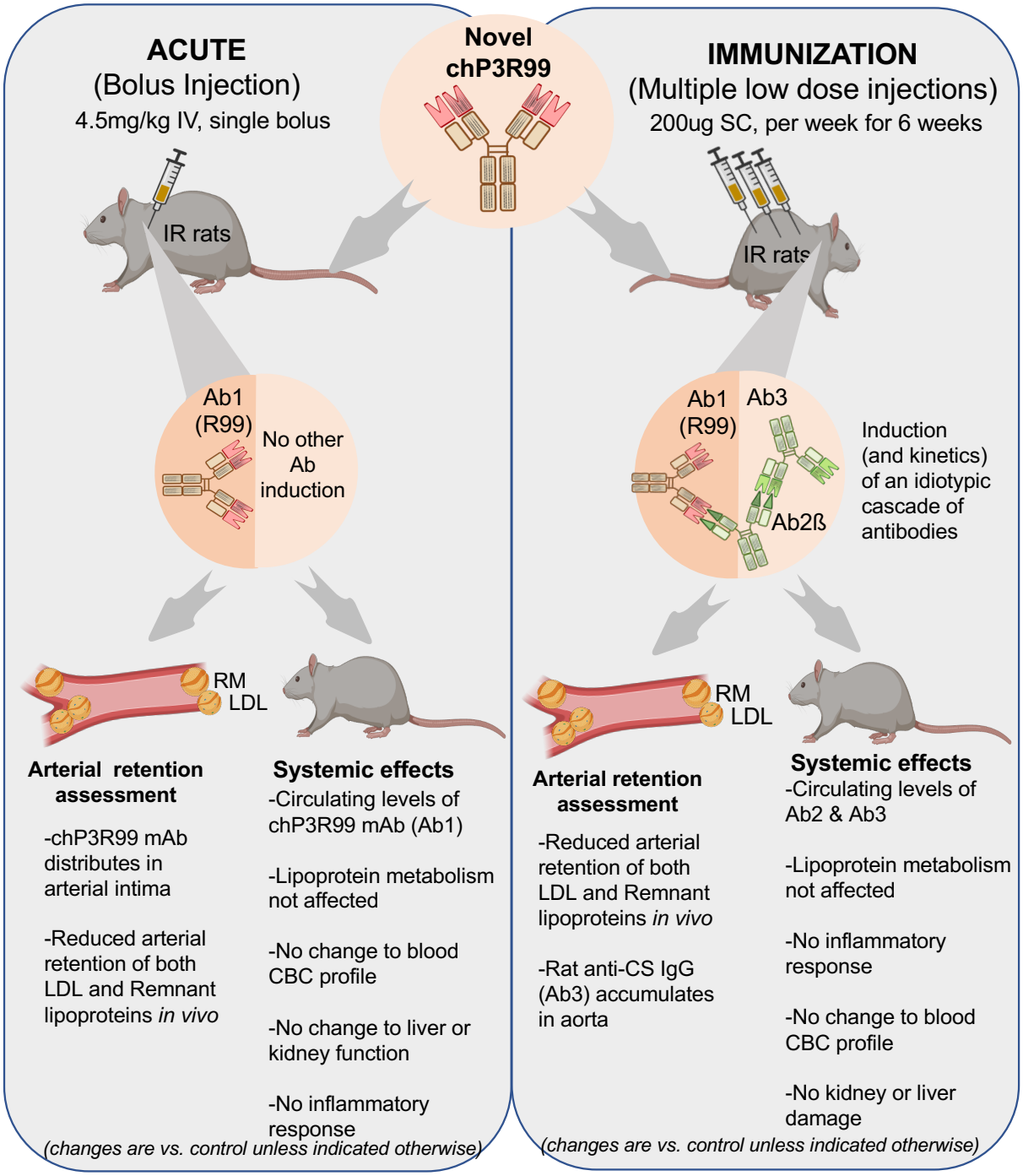

Abbreviations: chP3R99: Chimeric P3R99 antibody (R99), Ab1: Antibody 1 (chP3R99), Ab2: Antibody 2 (anti-chP3R99), Ab3: Antibody 3 (anti-CS), LDL: Low-density lipoproteins, IV: Intravenous, SC: Subcutaneous, IR: Insulin Resistance, CBC: Complete blood count, CS: Chondroitin Sulphate, IgG: Immunoglobulin G

INTRODUCTION

Atherosclerotic vascular disease (ASVD) afflicts millions of individuals each year, particularly those with insulin-resistance (IR) or diabetes (1,2). Despite the rapid discovery of new cholesterol and lipid lowering agents, the continued rise in the incidence of ASVD suggests that we are yet to completely understand the etiology of atherosclerosis. The 'response-to-retention' hypothesis for atherosclerosis suggests that lipid and cholesterol accumulate in arterial vessels derived from fasting and non-fasting lipoproteins (3-4). Atherogenic cholesterol-dense lipoproteins (for example low density lipoprotein, LDL) are thought to permeate both intact and/or damaged arterial endothelium, become entrapped within the sub-endothelial space and accumulate, resulting in inflammation and atheroma (3-4). Although the literature documents a significant epidemiological and/or genetic (i.e. GWAS) association between raised circulating fasting LDL cholesterol (LDL-C) and ASVD risk, a large proportion of subjects diagnosed with ASVD are either normolipidemic (normal levels of LDL-C), or have substantial residual risk (5-7). These data suggest that clinically, atheromata-associated cholesterol is derived from alternate sources, including non-fasting remnant (RM) lipid fractions (8).

In support of this concept, a series of publications authored by the Copenhagen Heart Study group (as well as others) have provided evidence for a major shift in the paradigm of atherogenesis (and potentially its therapy), suggesting that remnant (non-fasting) cholesterol is a major causative factor for ASVD (9-13). These clinical outcomes have caused us to refine our focus to how we might therapeutically target remnant cholesterol. Traditional therapeutic strategies have focused on the modulation of risk factors for ASVD (i.e. lipid lowering) rather than halting lipoprotein retention in the artery wall *per se.* Importantly, there have been key contributions to this field (by us and others) (14-19), that provide proof of principal that targeting the interaction of both LDL and RM lipoproteins specifically within the arterial wall is a unique and viable therapeutic strategy to reduce atherosclerosis.

Histological examination of arterial proteoglycan (PG) distribution in human tissue with ASVD has demonstrated increases in chondroitin sulfate (CS) PGs like biglycan, decorin and versican compared to vessels without disease (20,21). The literature also documents that the capacity for PG-associated glycosaminoglycans (GAGs) to bind LDL (as well as RMs) is related to the electrostatic properties and length of their side chains (22-27).

To complicate matters, we also now appreciate that the condition of insulin resistance (IR) is a critical precursor to Type-2 diabetes with the sequelae to ASVD (27-30). We know that chronic IR results in changes in arterial architecture, vascular perturbations, and dyslipidemia. Vascular dysfunction is associated with IR can re-model (stimulate) extracellular arterial CSPGs and intimal thickening (27-30). Excessive proliferation of vascular SMCs can stimulate the secretion of arterial CSPGs, which in turn increases the capacity for lipoprotein binding (27-32). Several lines of evidence suggest that this produces a unique sulfation pattern on arterial GAGs during ASVD, propagated by TGF-β (33-36).

The interaction of atherogenic lipoproteins with arterial PG offers an explicit target for atherogenesis, but the technological capacity for this approach has not been viable until now. For this study we proposed to utilize a highly innovative monoclonal antibody (mAb) chP3R99 (made possible by a collaboration with the Centro de Inmunología Molecular (CIM), Cuba). Investigators at CIM have pioneered the development of a highly unique mAb that recognizes sulfated GAGs found within CSPGs (38-40) (Figure 1). The chP3R99 mAb has been demonstrated to interfere directly with the interaction of LDL to CS *in vitro* and markedly reduces the retention of LDL *in vivo* (37-40). Importantly, the chP3R99 has been shown to accumulate in lesion areas *in vivo* (41). These advancements suggest a high degree of specificity for CS within arterial lesions and reduced affinity for other enriched sites; suggesting specificity for a unique CS sulfation expressed on vascular GAGs (37-41). For this study we proposed (i) that the chP3R99 mAb would interfere (acutely) with both LDL and RM lipoproteins both *in vitro* and *in vivo*; and (ii) that vaccination with chP3R99 in rodent model of IR would similarly reduce overall retention of lipoproteins but be associated with the production of 2nd and 3rd Ab responses consistent with an idiotypic cascading effect (42).

METHODS

Antibodies

ChP3R99 (Figure 1) and hR3 (anti-human epidermal growth factor receptor) mAbs were provided by the Center of Molecular Immunology (Havana, Cuba). As per previous published studies, the mAbs were purified by protein-A affinity chromatography (Pharmacia, Sweden) from transfectome culture supernatants and analyzed by SDS-PAGE under reducing conditions (37, 38). The specificity of the purified mAbs was confirmed by enzyme-linked immunosorbent assay (ELISA) and protein concentration was estimated by optical density at 280 nm. In all set of experiments, an Ab variant with impaired capacity to bind Fc gamma receptor (FcγR) and the complement system was used to avoid undesired Fc-mediated pro-inflammatory effects (chP3R99-LALA, referred to as chP3R99 subsequently).

Animal model

Experiments in animals were conducted in JCR:LA-cp (cp/cp) male rats (400-600 g), a spontaneously recessive strain with an absence of the leptin receptor leading to hyperphagia-associated obesity, along with severe IR. As a metabolically normal control, age-matched lean (+/cp) rats (350-400 g) from the same strain fed a chow diet throughout the studies were used. The rats were raised in our well-established colony at the University of Alberta (Edmonton, Canada) under standard conditions (25°C, 60±10% humidity), 12 h day/night cycles with water and food *ad libitum* (16). All experiments were conducted as per the Canadian Council for Animal Care (CCAC) and approved under the University of Alberta protocol numbers AUP000952 and AUP0004174.

Arterial perfusion experiments and general study design(s)

Acute perfusion experiments with the mAbs were conducted at 12 weeks of age in IR rats fed a chow diet as previously described (14-16). For subsequent experiments, 10-week-old IR rats were submitted to a lipid-balanced diet supplemented with 1% w/w cholesterol for six weeks (43). Physiological studies to address potential toxicity of chP3R99 administration were conducted both in lean control and IR rats. In the acute experiments, the rats received a bolus IV injection of the mAbs at 4.5 mg/kg in PBS through the jugular vein at 15 weeks of age. Conversely, to assess the impact of the vaccination with this mAb, the rats were given

six SC injections of P3R99 mAb (200 µg, once a week), hR3 isotype control or saline (n=6) along with the high fat diet feeding. In both settings, blood samples were drawn at different time points for further analysis in sera and plasma. Also, a complete blood count was carried out before starting the treatment with the mAbs and at the endpoint by mean of a Coulter STKS instrument (Coulter Electronics). The animals were fasted overnight, anesthetized under 3.5% isofluorane-oxygen for surgical procedures and sacrificed by exsanguination. Tissue samples were collected appropriately for histopathological, immunofluorescence, immunoblotting and biochemical evaluations.

Lipoprotein preparations

Intestinal RM lipoproteins were isolated and labeled with fluorophores following a methodology as previously described (14-16). Chylomicrons were labeled with Cy5 according to manufactures instructions (GE Healthcare UK limited, Buckinghamshire, UK) and injected into hepatectomized rabbits (n=3) to obtain RM endogenously (14-16). The later were isolated from rabbit sera by ultracentrifugation, whereas human LDL were obtained commercially and labeled with Cy3 (Millipore Sigma Canada Ltd, ON, Canada). Previous studies have demonstrated that ApoB48-Cy5 and ApoB100-Cy3 are not transferred between lipoproteins and do not have altered clearance from plasma, or organ uptake (14-15).

Confocal analysis

The arterial retention of lipoproteins was quantified by a previously established method that measures the total fluorescent intensity obtained by confocal microscopy of at least five carotid sections per animal (Olympus IX-8 Perkin Elmer spinning disk microscope) (14-16). The volume of each section was calculated based on the area (determine by the elastin autofluorescence at 495 nm), the number of sections per animal, and the interval between 10 Z-sections analyses per slice. The total fluorescence intensity of the perfusate (532 nm for Cy3-LDL and 635 nm for Cy5-RM) per unit volume was also collected for every experiment, under identical conditions in Z-series. Based on the corresponding number of apoB48/100 particles (using a known concentration of ApoB48/100 in a specific volume of the perfusate) as well as the corresponding concentration of cholesterol per particle (14-16).

Solid-phase assays

Recognition to CS and extracellular matrix

Recognition to CS was performed on amine-reactive 3D polymer-printed chamber slides (Nexterion Slide H, Schott Nexterion®, AZ, USA). The wells were incubated with 250 µL of the mAb solutions for 90 min at RT, diluted at 25 or 125 µg/mL in HBS containing 2 mmol/L $CaCl_2$ and 2 mmol/L $MgCl_2$ (sample buffer). Alternatively, the reactivity to extracellular matrix (ECM) derived from VSMC (44,45) was evaluated in Lab Tek Chambered slides. In this case, the plates were blocked with a 1% BSA solution in HBS for 1h at RT, followed by incubation with 400 µL of the mAb solutions (5-125 µg/mL) in sample buffer for 1h at RT (37). In both sets of experiments, the mAb reactivity was detected by mean of a Cy3-conjugated goat anti-human IgG serum (Jackson Immunoresearch Laboratories, West Grove, PA), diluted 1:1000 in 0.1% BSA in HBS, and incubated for 90 mins at RT. Finally, the chamber separators were removed, and the slides were scanned at 532 nm (GenePix 4000B, San Jose, CA). Specificity was assessed using hR3 mAb as isotype-matched control.

Immunogenicity of chP3R99 mAb in rats

The capacity of chP3R99 mAb (Ab1) to induce an idiotypic cascade of Abs in rats was evaluated by ELISA, based on a previous approach (46) (Figure 1). Briefly, the kinetics of induction of anti-idiotypic Abs (Ab2 response) and anti-anti-idiotypic Abs (Ab3 response, autologous anti-CS rat Abs), both in IR and control rats immunized with this mAb. All the assays were performed in triplicate for each condition and the coefficient of variation was <10%. Background values were less than 0.1.

Quantitative ELISA

The content of human IgG was quantitated both in the sera and aortic (tissue) homogenates from rats treated with chP3R99 or hR3 mAbs by a commercial ELISA kit (Sigma-Aldrich). Similarly, haptoglobin (ALPCO, NH, USA), aspartate aminotransferase (AST) and alanine transaminase (ALT) (Elabscience, TX, USA), and β2-microglobulin (Novus Biologicals, CO, USA) were quantified in plasma collected at the ending time following the instructions provided by the manufacturers.

Immunoblot analysis

Activated Immobilon-P PVDF membranes (Millipore Sigma, ON, Canada) spotted with decorin or biglycan (20 µg/well) were blocked with a 5% skim powder milk solution in 0.1%

Tween 20-containing tris-buffered saline (TBST) [50 mM Tris HCl (pH 7.5), 150 mM NaCl]. The membranes were incubated ON at 4°C in agitation with the rat tissue homogenates from immunized rats at a protein concentration of 1.5 mg/mL in the blocking buffer. After washing three times with TBST for 15 min, membranes were incubated for 1 h at RT with HRP-conjugated anti-human IgG or anti-rat IgG secondary Abs (Jackson) diluted in blocking buffer. The reaction was visualized by chemiluminescence using ECL Advance Western Blotting Detection kit (GE HealthCare) and the dots quantified using ImageJ NIH software (version 1.50i).

Postprandial studies and lipid analysis

Postprandial studies were conducted in rats at 15 weeks of age, 24 h after bolus injection of the mAbs (n=3 per group) or a week after the fifth immunization (n=6 per group). After fasting ON, rats were subjected to an oral fat challenge as described elsewhere (17). Blood samples were drawn from the tail at times 0, 2, 4, 5, 6 and 8 h following consumption of the pellet meal. Plasma TG, total cholesterol (TC), LDL cholesterol and high-density lipoproteins (HDL) cholesterol were determined both in postprandial and fasting plasma samples by colorimetric assays (Wako, Chemicals USA Inc., Richmond, VA). Also, TG and TC were quantified in liver homogenates by colorimetric assays (Wako). The concentration of TG and Total cholesterol were measured by ELISA using an aliquot of the whole homogenate and adjusted by the protein concentration of the homogenate (17).

Cytokine quantification

Cytokines, growth factors, leptin and the C-reactive protein (CRP) were quantified by multiplex immunofluorescence assays by the company Eve Technologies (Calgary, AB, Canada) in aortic homogenates from rats and/or plasma.

Histological and Immunofluorescence studies

Histological studies were performed in fresh-frozen tissue sections (5 µm) stained with hematoxylin-eosin and Oil red O-stained liver sections (10 µm). To assess the accumulation of chP3R99 mAb in different organs, tissue sections were incubated with a goat FITC-conjugated anti-human IgG serum (Jackson) and counterstained with Hoechst. Images were

digitally captured with a DP20 camera coupled to a fluorescence microscope Olympus BX51. And the images quantified (ImageJ 1.50i).

Statistical analysis

Statistical analysis was performed in GraphPad Prism 7 (GraphPad Software, Inc). Results are expressed as mean±SEM unless otherwise stated. Unpaired t-test or one-way analysis of variance (ANOVA) for multiples comparisons followed by Bonferroni post-test were used accordingly. For postprandial studies, the area under the curve was determined by the trapezoidal method with NCSS™ GraphPad (17). Values of $p<0.05$ were considered statistically significant. The significance levels are shown in the figures and the legends of the figures and tables.

RESULTS

ChP3R99 mAb recognizes vascular extracellular matrix inhibiting subendothelial lipoprotein retention in insulin-resistant rats

Solid-phase *in vitro* studies confirmed the capacity of chP3R99 mAb to recognize CS (Figure 2A) and demonstrated specific, dose-dependent binding to the ECM secreted by VSMC (Figure 2B). Previous studies have demonstrated that chP3R99 mAb competes with LDL for the binding site on sulfated GAG sugar chain of PG (41). Here we hypothesized that the chP3R99 mAb would interfere with the arterial retention of both LDL and RM lipoproteins. Figure 2C-D shows that the binding of LDL to CS and the ECM *in vitro* was approximately 3.5-fold greater than for RM. In this setting, chP3R99 reduced the interaction of both LDL and RM with either CS (Figure 2C) or the vascular ECM (Figure 2D, $p<0.001$). While the absolute reduction of the number of LDL particles resulting from the addition of chP3R99 mAb was greater than for RM, the corresponding proportion of cholesterol-reduction was similar between the two lipoprotein preparations (Figure 2E-F, $p<0.05$). We also verified these results using VSMC cultured in hyperglycemic conditions in the presence of insulin (Supplemental Figure IA-C).

The findings *in vitro* prompted us to investigate whether chP3R99 could impinge the arterial retention of RM under physiological conditions. As a first approach, carotid arteries from IR rats were pre-perfused (*in situ*) with chP3R99 mAb at a concentration of 125 µg/mL, followed by the perfusion of pre-labelled RM only at 90 µg/mL. Presence of chP3R99 significantly reduced the retention of both the number of RM particles in arterial vessels (~65%) as well as the corresponding deposition of RM-associated cholesterol (Figure 3A, C, $p<0.05$). We also observed a dose-dependent capacity (25-250 µg/mL) of the chP3R99 mAb to inhibit arterial retention of RM lipoproteins *in vivo* (Figure 3D and Supplemental Figure IIA) as well as the corresponding deposition of cholesterol (Figure 3E, $p<0.001$). Unlike the isotype control mAb, abundant accumulation of chP3R99 *per se* was visualized in carotids from IR rats, in areas void of RM (Figure 3F).

Interestingly, *ex-vivo* (competitive) perfusion of equivalent amounts of both LDL and RM in carotids from IR rats resulted in significantly higher retention of ApoB100 (2.8-fold) and ApoB48 (3.6-fold) respectively, relative to lean controls (Figure 3G). Pre-perfusion with

chP3R99 reduced the retention of both LDL (60%) as well as RM (32%). Despite the lower retention of the latter, its contribution to cholesterol deposition in the carotids was greater than for LDL ($p<0.05$) (Figure 3H). Also of note is that we employed a ratio of ApoB/P3R99 (90 µg/mL: 125 µg/mL respectively) to assess the blocking capacity of P3R99 on RM retention relative to LDL (non-saturating conditions in which the mAb elicit approximately 50% inhibition for LDL).

Vaccination with chP3R99 mAb reduces the arterial retention of pro-atherogenic lipoproteins in IR rats

A unique property of the chP3R99 mAb is the immunogenicity of its idiotypic region (involved in antigen recognition), able to induce anti-sulfated GAG Abs *in vivo* (40,42). Here we evaluated the immunogenicity of chP3R99 in JCR:LA-*cp* rats (Figure 4A), along with the impact of the vaccination approach. Short-term immunization with chP3R99 mAb also resulted in a reduction of the retention of LDL and RM in the carotids of IR rats (Figure 4B). Quantitative analysis demonstrated a lower content of ApoB100 (~30%) and ApoB48 (~40%) in the artery wall and the associated ApoB-cholesterol (Figure 4C-D, $p<0.01$).

Kinetic experiments revealed that chP3R99 mAb (but not the isotype control), mounted a strong anti-idiotypic (Ab2) response in rats after a second injection of the mAb, which was very similar between wildtype and IR rats (Figure 4E). Interestingly, anti-CS Abs (Ab3 response) were detected in sera three weeks after the first mAb injection in the lean controls while requiring an additional week for IR rats. Overall, the levels of anti-CS Abs were higher in the sera of lean rats when compared with IR rats (Figure 4F). We also found an induction of anti-dermatan sulfate Abs and a low response against the unsulfated GAG hyaluronic acid in rats (data not shown).

Since the immunogenicity of chP3R99 appeared similar in lean and IR rats, we hypothesized that lower circulating levels of anti-CS Abs in the later could be related to the accumulation in the arteries rather than an impaired production in IR rats. To address this, we developed an immunoblot technique in which both decorin and biglycan were spotted on membranes (as examples of proatherogenic CS/DS-containing PGs), followed by incubation with aorta homogenates. We detected the presence of autologous anti-PGs IgG (Ab3) generated by the immunization in aortic lysates from IR rats immunized with chP3R99 (Figure 4G-H) which was further confirmed by ELISA (Figure 4I). Despite the potential for chP3R99 to recognize

hepatic derived-PGs *in vitro*, neither this mAb (not shown) nor the autologous anti-CS Abs significantly accumulated in the liver (Figure 4I).

The treatment with chP3R99 did not affect the overall biochemical status of rats

Additional studies were conducted in lean and IR rats to address potential toxicity associated with a therapy directed to CS, not only in normal physiological conditions but also in a more compromised physiological status of IR. We analyzed clinical and biochemical parameters in rats immunized with chP3R99 (Figure 4A) or those who received a bolus IV injection of this mAb (Figure 5A).

First, we quantified the concentration of human IgG in plasma in each setting, as well as the immunogenicity of chP3R99, to elucidate any direct contribution of the Ab1 versus the one from autologous Ab3 on the overall physiological status of the rats. We detected circulating levels of the isotype control mAb by ELISA in the sera from lean controls (104.6±21.8 ng/mL) and IR rats (63.1±39.7 ng/mL) a week after the last immunization but not of chP3R99 mAb. Interestingly, while all groups had similar levels of circulating IgG after 24 h, IR rats receiving chP3R99 had significantly lower concentrations after one week (Figure 5B, $p<0.001$). Quantitative ELISA further demonstrated the presence of chP3R99 mAb in aorta homogenates from IR rats (10.6±1.0 ng/mg of protein) whereas immunofluorescence studies did not show any accumulation in other tissues. We also verified that, even at a high dose of chP3R99 mAb, one week was not sufficient to generate an idiotypic cascade (data not shown).

Classically, 16-week-old cholesterol-fed JCR:LA-cp rats were characterized by significantly higher levels of leptin (153.1±13.8 vs 34.7±2.6 µg/mL, $p<0.0001$), obesity (584.5±10.2 vs 337.5±10.1 g, $p<0.0001$) and dyslipidemia (Table I and Figure 5), relative to age-matched control rats (Supplemental Table I). Importantly, the body weight was not affected throughout the treatments. Although no significant fasting hyperglycemia was observed ($p>0.05$), extremely high levels of insulin were detected (1228.0±84.3 vs 129.5±10.6 pmol/L, $p<0.0001$), confirming severe insulin resistance as indicated also by their HOMA-IR index (Table I). Likewise, IR rats showed significantly higher levels of AST and ALT than the lean controls ($p<0.01$), measured as indicators of liver damage. Plasma concentration of β2-microglobulin, a surrogate marker of kidney damage, was also significantly increased in IR

rats ($p<0.01$). None of the parameters mentioned above were affected by the treatment with chP3R99 (Table I and Supplemental Table I). Neither the acute treatment with chP3R99 nor the immunization with chP3R99 affected the total blood cells counts in IR or lean control rats (Supplemental Tables II and III).

ChP3R99 mAb did not interfere with lipoprotein metabolism *in vivo*

The role of heparan sulfate PGs, particularly syndecan I, in the hepatic clearance of triglyceride-rich lipoprotein RM has been well established (47). To study in more detail whether a treatment based on chP3R99 mAb could affect lipoprotein metabolism we analyzed plasma TG and cholesterol levels at different time points, both in fasting conditions and in the postprandial state (Figure 5 and Table I).

In fasting samples (Figure 5C), IR rats under high-fat diet displayed higher levels of plasma TG (mainly associated with the chylomicron/VLDL and HDL fractions) relative to the lean controls. Total cholesterol was also elevated in those rats but mostly distributed in HDL and less extensive in the chylomicron/VLDL fraction. Importantly, the bolus administration of chP3R99 mAb did not modify the lipid profile of IR or lean rats when compared with the isotype-matched control 24 h or a week after the mAb administration. Similar results were observed in the rats immunized with chP3R99 mAb. Further assessment of TG and cholesterol associated with different lipoprotein classes confirmed no difference between the groups treated with chP3R99 and their corresponding control groups (Table I, $p>0.05$).

Assessment under the postprandial state (Figure 5D) revealed that the IV inoculation of chP3R99 had no impact on plasma concentrations of either TG or cholesterol after submitting the rats to a fat challenge. Interestingly however, IR rats immunized with chP3R99 showed significantly lower postprandial TG-AUC relative to hR3-receiving rats (AUC=2071 *vs* 3157, $p<0.05$). Oil red O staining of liver sections also confirmed steatosis in IR rats but no difference in the accumulation of neutral lipids between chP3R99-treated rats and the control groups was observed (Figure 5E).

ChP3R99 mAb did not alter the inflammatory status of the insulin-resistant rats

Unlike CRP, which was similar in all the groups, plasma levels of haptoglobin were significantly higher in IR rats compared to lean controls (10.9±1.9 vs 3.6±0.5 mg/mL, $p=0.008$). Interestingly, a 3-fold reduction in the concentrations of haptoglobin was observed

in IR rats who received an acute administration of chP3R99 (Table I), while showing no effect in the lean control group or any of the immunized rats (Table I and Supplemental Table IV). As expected, we verified a low grade systemic inflammatory condition in IR rats relative to control (Table II); characterized by increased levels of IL-6 ($p<0.0001$) and of IFN-γ, TNF-α, IL-2, G-CSF and RANTES ($p<0.05$). However, no significant difference was observed between any of the mAb-treated groups in IR rats treated acutely with chP3R99 mAb.

A similar cytokine array performed in aorta homogenates showed no differences between any of the groups ($p>0.05$) for the variables that were possible to accurately detect in those samples (Data not shown).

DISCUSSION

Epidemiological and Mendellian Randomization studies in Europe, North America and now other countries (9-13), support the notion that RM lipoproteins (measured as RM cholesterol), have substantial independent contributions to CVD risk; and that these relationships maybe stronger than for LDL-C under conditions of residual risk and/or diabetes. There is certainly a plethora of pre-clinical evidence demonstrating the interaction of both LDL and RM lipoproteins within the arterial wall (3, 4, 8, 14-20), consistent with the response-to-retention hypothesis and attachment via select CS arterial PGs (3, 4, 8, 20-23). Limited case control studies have shown similar observations in human vascular tissue (20, 21, 48, 49). In order to advance our understanding of not only the contribution of these atherogenic lipoproteins, but to develop a potential therapeutic to interfere directly with the deposition of cholesterol, we sought to assess the efficacy of the novel chP3R99 mAb both *in vitro* and *in vivo.*

Novel target of chP3R99 mAb

The Centro de Inmunología Molecular (CIM), Cuba originally developed the murine P3 mAb devised to recognize N-glycolilated gangliosides and sulfatides (50). The P3 mAb was characterized with the unusual property of generating a strong anti-idiotypic response when administered in syngeneic animal models (even in the absence of adjuvants or carrier proteins) (51). A second generation of the mAb was engineered to produce a chimeric mouse/human IgG1 variant of P3 (chP3) that was shown to retain the specificity and idiotypic immunogenicity (52, 53). Subsequently, a chP3 mutant was engineered with an additional arginine in position 99 at the Complementarity-determining Region 3 (H-CDR3) from the heavy chains (Kabat numbering; chP3R99), that displayed an even higher reactivity with antigens, especially sulfatides (54). Finally, the Fcγ receptor and complement-binding region of the chP3R99 mAb was refined to impair undesired induction of inflammatory response (i.e. chP3R99-LALA) (Figure 1A) (37). The chP3R99 mAb and the control hR3 continue to be generated at the CIM (54, 55). It has previously been reported that chP3R99 has the capacity to interfere with the development and progression of atherosclerosis in mice and rabbit models (37-39, 46). In an extension to this work, we now demonstrate that chP3R99 can interfere with the interaction of both LDL and RM lipoproteins to vascular regions susceptible to atherogenesis in a rat model of IR.

Idiotypic characteristics of chP3R99 mAb

The chP3R99 has been developed as a unique mAb that recognizes sulfated GAGs found within the (CS) family of PGs (37-39, 56, 57). In addition to antigen recognition mediated by the complementarity-determining region (CDR) motifs of the P3 idiotype, the region contains both $CD4^+$ and $CD8^+$ T-cells epitopes, conferring a high immunogenicity which is preserved in chP3R99 mAb. The idiotope is a generic 'structural' term given to unique sequence of antigenic determinants (epitopes) located on the variable portion of any given Ab. An 'anti-idiotype' Ab [2nd generation-Ab2], in turn, is specific for an Ab1 idiotope and may resemble the 3D structure of the antigen (Ab2β, also known as 'internal image' of the antigen) as described in the cascading 'immune network theory' originally proposed by Nobel Laureate Niels Jerne (reviewed in 42). The 'anti-idiotypic response' is thought to explain the amplification of a highly specific region of the 'original' idiotype and acts as a vaccine to provide long-term recognition (Figure 1B).

The therapeutic potential of the chP3R99 idiotypic mAb is two-fold; (i) acute recognition to the antigen, specifically its idiotype (in this case interfering with ApoB-GAG-complex formation), and (ii) vaccination with the mAb (chronic response) mounts an autologous 'cascade' of Abs that reproduce the specificity of the original mAb, amplifying antigen recognition analogous to a vaccine. In this study we not only show that the chP3R99 mAb recognizes vascular ECM inhibiting subendothelial lipoprotein retention (acutely) in IR rats, but also that the 'vaccination' with the same, also can interfere with arterial retention of pro-atherogenic lipoproteins over time. Indeed, we have also been able to demonstrate the immunogenicity of chP3R99 inoculation in rats to develop not only Ab2, but Ab3 antibodies. Our kinetic experiments revealed that chP3R99 mAb mounted a strong anti-idiotypic (Ab2) response in rats after a second injection of the mAb, (similar in wildtype and IR rats). Interestingly, the detection of an Ab3 response in sera was delayed compared to the appearance of Ab2, indicating that the latter may be essential to induce an anti-CS response or activate/amplify a natural response against this antigen. Perhaps more interesting, was that the anti-CS Abs (Ab3 response) in IR rats was 1 week slower than for lean control wildtype rats; and overall, Ab levels did not reach the maximum response observed in control rats. It might be plausible that under systemic low grade inflammatory conditions the strength of the idiotypic response to chP3R99 may be impaired. However, the presence of a comparable Ab2

response, in both immunocompromised and normal conditions, suggests that the anti-CS Abs generated in IR rats could be accumulating in the arteries. Indeed, we were able to demonstrate, for the first time, that the autologous anti-CS Abs accumulate in aorta and associated with reduced lipoprotein retention *in vivo*. Other unpublished data from our group suggests that as few as two SC injections of P3R99 (50 µg) are sufficient to interfere (reduce) aortic lipoprotein retention in Sprague-Dawley rats following a bolus administration of LDL. To our knowledge, the specific accumulation of Ab3 in the targeted organ has not been previously reported (as opposed to the detection Ab3 in sera or characterized *in vitro*)(58).

The clinical approach to the idiotypic theory has primarily relied on anti-idiotypic vaccines (Ab2 mAbs) (58), whereas chP3R99 mAb is an Ab1 capable of mounting a full idiotypic cascade. This unique characteristic not only enables chP3R99 to directly recognize CSPGs, but also opens the potential for its use as a passive therapy, a vaccine, or a combination of both strategies. Thus, the potential of this mAb in clinical applications extends beyond the direct antigen recognition amplifying its specificity through an idiotypic cascade mechanism. While idiotypic/anti-idiotypic vaccines hold potential for targeting various antigens, a significant portion of the clinical applications explored so far have focused on carbohydrates and glycolipids, primarily in the field of cancer immunotherapy (summarized in 58). While carbohydrates are known for their poor immunogenicity, the fact that Ab2 resemble the antigens offer a promising strategy for mimicking those molecules (ie: GAG) within a protein framework, thereby potentially eliciting a more effective immune response.

Future studies should now consider larger and higher order animal models to ensure that chronic inoculations of chP3R99 are sufficiently immunogenic in clinically translatable immune systems.

Developmental limitations of chP3R99 mAb

The development of a putative mAb to target vascular lipoprotein interactions does not come without theoretical limitations. The biological purpose of CSPGs is not limited to structural integrity of the vasculature. The biological function of the four main PGs families is known to be expressed throughout physiology in extracellular, pericellular, cell surface and intracellular regions (59). The putative interaction of a mAb to each or any of these 'on-target but off-vasculature' sites would claim additional properties to impair functional (and/or structural) biochemical processes (hepatic HSPGs), compete with normal metabolic

pathways (lipid metabolism) and plausibly stimulate inflammatory cascades. However, it is also notable that GAG composition in peripheral tissues is often modified in numerous pathologies, including ACVD and cancer. In atherosclerosis, CSPGs are predominantly synthesized by VSMCs, resulting in distinctive features such as enlarged GAG chains, increased sulfation, along with changes in the sulfation pattern (60).

In this study (using rats), we have not been able to identify any significant biochemical signal that could be interpreted to be associated with any negative attribute of the chP3R99 mAb. Indeed, all studies that have utilized the chP3R99 mAb to date, have not reported any systemic 'on-target' but off-vasculature' effects including those in mice, rats and rabbits. To the contrary, there has been enticing data collected using immunoscintigraphy by intravenous administration of ^{99m}Tc-chP3R99 mAb in atherosclerotic and control rabbits (41). The overall uptake of ^{99m}Tc-chP3R99 mAb was predominantly localized in liver, kidneys and heart alongside all time intervals. However, the planar images acquisition revealed the accumulation of ^{99m}Tc-chP3R99 mAb in the carotid of atherosclerotic rabbits 6 h after radiotracer administration, but not in control animals. Future studies will need to continue to explore various and reproducible ways of demonstrating inert clearance mechanisms of the active and inactive mAbs.

CONCLUSION

Acute and long-term inoculation of chP3R99 mAb interfered with the interaction of both LDL and RM lipoproteins with arterial PGs in a setting of IR. These *in vivo* data support the innovative approach of targeting pro-atherogenic lipoprotein retention by this mAb as a passive therapy or as an idiotypic vaccine for atherosclerosis.

ACKNOWLEDGEMENTS:

We are grateful for the technical expertise provided by Ms. Sandra Kelly and Sharon Sokolik.

SOURCES OF FUNDING:

Funds for this work were provided in part by the following sources; a grant in aid from the Heart and Stroke Foundation of Canada to S. Proctor, a project grant from the Canadian Institutes for Health Research to S. Proctor. Dr. Soto was supported by an International Atherosclerosis Society fellowship award.

DISCLOSURES:

Dr. Soto, Dr. Brito, and Dr. Vazquez are inventors of a patent related with antibodies that recognize sulfatides and sulfated proteoglycans. However, they have assigned their rights to the Center of Molecular Immunology.

REFERENCES

1. Caballero AE. Metabolic and vascular abnormalities in subjects at risk for type 2 diabetes: the early start of a dangerous situation. *Arch Med Res*. 2005;36(3):241-9.
2. Eckel RH, Grundy SM, Zimmet PZ. The metabolic syndrome. *Lancet*. 2005;365(9468):1415-28.
3. Williams KJ, Tabas I. The response-to-retention hypothesis of early atherogenesis. *Arterioscler Thromb Vasc Biol*. 1995;15(5):551-61.
4. Borén J, Williams KJ. The central role of arterial retention of cholesterol-rich apolipoprotein-B-containing lipoproteins in the pathogenesis of atherosclerosis: a triumph of simplicity. Curr Opin Lipidol. 2016 Oct;27(5):473-83. PMID: 27472409.
5. LIPID Study Group (Long-term effectiveness and safety of pravastatin in 9014 patients with coronary heart disease and average cholesterol concentrations: the LIPID trial follow-up). *Lancet.* 2002;359(9315):1379-87.
6. Mediene-benchekor S, Brousseau T, Richard F, Benhamamouch S, Amouyel P. Blood lipid concentrations and risk of myocardial infarction. *Lancet.* 2001;358(9287):1064-5.
7. Colhoun HM, Betteridge DJ, Durrington PN, et al. Primary prevention of cardiovascular disease with atorvastatin in type 2 diabetes in the Collaborative Atorvastatin Diabetes Study (CARDS): multicentre randomised placebo-controlled trial. *Lancet.* 2004;364(9435):685-96.
8. Zilversmit DB. Atherogenic nature of triglycerides, postprandial lipidemia, and triglyceride-rich remnant lipoproteins. *Clin Chem.* 1995;41(1):153-8.
9. Varbo A, Benn M, Tybjærg-hansen A, Jørgensen AB, Frikke-schmidt R, Nordestgaard BG. Remnant cholesterol as a causal risk factor for ischemic heart disease. *J Am Coll Cardiol.* 2013;61(4):427-36.
10. Varbo A, Benn M, Smith GD, Timpson NJ, Tybjaerg-hansen A, Nordestgaard BG. Remnant cholesterol, low-density lipoprotein cholesterol, and blood pressure as mediators from obesity to ischemic heart disease. *Circ Res.* 2015;116(4):665-73.
11. Nordestgaard BG, Langsted A, Mora S, et al. Fasting is not routinely required for determination of a lipid profile: clinical and laboratory implications including flagging at desirable concentration cut-points-a joint consensus statement from the

European Atherosclerosis Society and European Federation of Clinical Chemistry and Laboratory Medicine. *Eur Heart J*. 2016;37(25):1944-58.

12. Weaver OR, Krysa JA, Ye M, Vena JE, Eurich DT and Proctor SD. Non-fasting remnant cholesterol and cardiovascular disease risk prediction in Albertans: a prospective cohort study. *CMAJ Open.* 2023 Jul 25;11(4):E645-E653.
13. Navarese EP, Vine D, Proctor S, Grzelakowska K, Berti S, Kubica J, Raggi P. Independent Causal Effect of Remnant Cholesterol on Atherosclerotic Cardiovascular Outcomes: A Mendelian Randomization Study. *Arterioscler Thromb Vasc Biol.* 2023 Sep;43(9):e373-e380.
14. Proctor SD, Vine DF, Mamo JC. Arterial permeability and efflux of apolipoprotein B-containing lipoproteins assessed by in situ perfusion and three-dimensional quantitative confocal microscopy. *Arterioscler Thromb Vasc Biol.* 2004;24(11):2162-7.
15. Proctor SD, Mamo JC. Intimal retention of cholesterol derived from apolipoprotein B100- and apolipoprotein B48-containing lipoproteins in carotid arteries of Watanabe heritable hyperlipidemic rabbits. *Arterioscler Thromb Vasc Biol*. 2003;23(9):1595-600.
16. Mangat R, Warnakula S, Borthwick F, et al. Arterial retention of remnant lipoproteins ex vivo is increased in insulin resistance because of increased arterial biglycan and production of cholesterol-rich atherogenic particles that can be improved by ezetimibe in the JCR:LA-cp rat. *J Am Heart Assoc*. 2012;1(5):e003434.
17. Vine DF, Takechi R, Russell JC, – SD. Impaired postprandial apolipoprotein-B48 metabolism in the obese, insulin-resistant JCR:LA-cp rat: increased atherogenicity for the metabolic syndrome. *Atherosclerosis.* 2007;190(2):282-90.
18. Mangat R, Su J, Scott PG, Russell JC, Vine DF, Proctor SD. Chylomicron and apoB48 metabolism in the JCR:LA corpulent rat, a model for the metabolic syndrome. *Biochem Soc Trans*. 2007;35(Pt 3):477-81.
19. Proctor SD, Vine DF, Mamo JC. Arterial retention of apolipoprotein B(48)- and B(100)-containing lipoproteins in atherogenesis. *Curr Opin Lipidol*. 2002;13(5):461-70.

20. O'brien KD, Olin KL, Alpers CE, et al. Comparison of apolipoprotein and proteoglycan deposits in human coronary atherosclerotic plaques: colocalization of biglycan with apolipoproteins. *Circulation.* 1998;98(6):519-27.
21. Nakashima Y, Wight TN, Sueishi K. Early atherosclerosis in humans: role of diffuse intimal thickening and extracellular matrix proteoglycans. *Cardiovasc Res.* 2008;79(1):14-23.
22. Flood C, Gustafsson M, Richardson PE, Harvey SC, Segrest JP, Borén J. Identification of the proteoglycan binding site in apolipoprotein B48. *J Biol Chem.* 2002;277(35):32228-33.
23. Williams KJ. Arterial wall chondroitin sulfate proteoglycans: diverse molecules with distinct roles in lipoprotein retention and atherogenesis. *Curr Opin Lipidol.* 2001;12(5):477-87.
24. Tannock LR, Little PJ, Wight TN, Chait A. Arterial smooth muscle cell proteoglycans synthesized in the presence of glucosamine demonstrate reduced binding to LDL. *J Lipid Res.* 2002;43(1):149-57.
25. Olsson U, Ostergren-lundén G, Moses J. Glycosaminoglycan-lipoprotein interaction. *Glycoconj J*. 2001;18(10):789-97.
26. Little PJ, Ballinger ML, Osman N. Vascular wall proteoglycan synthesis and structure as a target for the prevention of atherosclerosis. *Vasc Health Risk Manag.* 2007;3(1):117-24.
27. Mangat R, Su JW, Lambert JE, Clandinin MT, Wang Y, Uwiera RR, Forbes JM, Vine DF, Cooper ME, Mamo JC, Proctor SD. Increased risk of cardiovascular disease in Type 1 diabetes: arterial exposure to remnant lipoproteins leads to enhanced deposition of cholesterol and binding to glycated extracellular matrix proteoglycans. *Diabet Med.* 2011 Jan;28(1):61-72.
28. Reaven G. Insulin resistance, type 2 diabetes mellitus, and cardiovascular disease: the end of the beginning. *Circulation.* 2005 Nov 15;112(20):3030-2.
29. Kraemer FB, Ginsberg HN. Gerald M. Reaven : Demonstration of the central role of insulin resistance in type 2 diabetes and cardiovascular disease. *Diabetes Care.* 2014;37(5):1178-81.
30. Tannock LR, King VL. Proteoglycan mediated lipoprotein retention: a mechanism of diabetic atherosclerosis. *Rev Endocr Metab Disord.* 2008;9(4):289-300.

31. Little PJ, Tannock L, Olin KL, Chait A, Wight TN. Proteoglycans synthesized by arterial smooth muscle cells in the presence of transforming growth factor-beta1 exhibit increased binding to LDLs. *Arterioscler Thromb Vasc Biol.* 2002;22(1):55-60.
32. S. P. Evanko, E. W. Raines, R. Ross, L. I. Gold, and T. N. Wight. Proteoglycan distribution in lesions of atherosclerosis depends on lesion severity, structural characteristics, and the proximity of platelet-derived growth factor and transforming growth factor-beta. *Am J Pathol.* 1998; 152(2): 533–546.
33. Rodriguez-Lee M, Bondjers G, Camejo G. Fatty acid-induced atherogenic changes in extracellular matrix proteoglycans. *Curr Opin Lipidol.* 2007;18:546-53.
34. Olsson U, Bondjers G, Camejo G. Fatty acids modulate the composition of extracellular matrix in cultured human arterial smooth muscle cells by altering the expression of genes for proteoglycan core proteins. *Diabetes.* 1999;48:616-22.
35. Figueroa JE, Vijayagopal P. Angiotensin II stimulates synthesis of vascular smooth muscle cell proteoglycans with enhanced low density lipoprotein binding properties. *Atherosclerosis.* 2002;162:261-8
36. Schonherr E, Jarvelainen HT, Kinsella MG, Sandell LJ, Wight TN. Platelet-derived growth factor and transforming growth factor-beta 1 differentially affect the synthesis of biglycan and decorin by monkey arterial smooth muscle cells. *Arterioscler Thromb*. 1993;13:1026-36
37. Soto Y, Acosta E, Delgado L, et al. Anti-atherosclerotic effect of an antibody that binds to extracellular matrix glycosaminoglycans. *Arterioscler Thromb Vasc Biol.* 2012;32(3):595-604.
38. Brito V, Mellal K, Portelance SG, et al. Induction of anti-anti-idiotype antibodies against sulfated glycosaminoglycans reduces atherosclerosis in apolipoprotein E-deficient mice. *Arterioscler Thromb Vasc Biol.* 2012;32(12):2847-54.
39. Delgado-roche L, Acosta E, Soto Y, et al. The treatment with an anti-glycosaminoglycan antibody reduces aortic oxidative stress in a rabbit model of atherosclerosis. *Free Radic Res*. 2013;47(4):309-15.
40. Delgado-roche L, Brito V, Acosta E, et al. Arresting progressive atherosclerosis by immunization with an anti-glycosaminoglycan monoclonal antibody in apolipoprotein E-deficient mice. *Free Radic Biol Med*. 2015;89:557-66.

41. Soto Y, Mesa N, Alfonso Y, et al. Targeting arterial wall sulfated glycosaminoglycans in rabbit atherosclerosis with a mouse/human chimeric antibody. *MAbs.* 2014;6(5):1340-6.
42. Vázquez AM, Rodrèguez-zhurbenko N, López AM. Anti-ganglioside anti-idiotypic vaccination: more than molecular mimicry. *Front Oncol.* 2012;2:170.
43. Wang Y, Lu J, Ruth MR, Goruk SD, Reaney MJ, Glimm DR, Vine DF, Field CJ, Proctor SD. Trans-11 vaccenic acid dietary supplementation induces hypolipidemic effects in JCR:LA-cp rats. *J Nutr.* 2008 Nov;138(11):2117-22.
44. Okada H, Nordt T, Lundgren CH, Fujii S. Human Aortic Vascular Smooth Muscle Cells Digest Extracellular Matrix by Elaboration of Plasminogen Activators: Implications for Atherogenesis. *J Thromb Thrombolysis.* 1995;2(2):107-112.
45. Sperti G, van Leeuwen RT, Quax PH, Maseri A, Kluft C. Cultured rat aortic vascular smooth muscle cells digest naturally produced extracellular matrix. Involvement of plasminogen-dependent and plasminogen-independent pathways. *Circ Res.* 1992 Aug;71(2):385-92.
46. Sarduy R, Brito V, Castillo A, Soto Y, Griñán T, Marleau S, Vázquez AM. Dose-Dependent Induction of an Idiotypic Cascade by Anti-Glycosaminoglycan Monoclonal Antibody in apoE$^{-/-}$ Mice: Association with Atheroprotection. *Front Immunol.* 2017 Mar 3;8:232.
47. Stanford KI, Bishop JR, Foley EM, Gonzales JC, Niesman IR, Witztum JL, Esko JD. Syndecan-1 is the primary heparan sulfate proteoglycan mediating hepatic clearance of triglyceride-rich lipoproteins in mice. *J Clin Invest.* 2009 Nov;119(11):3236-45.
48. Pal S, Semorine K, Watts GF, Mamo JCL. Identification of lipoproteins of intestinal origin in human atherosclerotic plaque. *Clin Chem Lab Med.* 2003 Jun;41(6):792-5.
49. Figueroa JGV, Sharma A, Rinehart S, Qian Z, Bhatt K, Joshi P, Pryor A, Blackman B, Teramoto T, Matsushima T, Kinoshita M, Voros S. First demonstration that hepatic APOB100 and intestinal APOB48 co-localize with macrophages in human carotid atherosclerosic plaques. *JACC.* March 27, 2012;59 (13).
50. Vazquez AM, Alfonso M, Lanne B, Karlsson KA, Carr A, Barroso O, Fernandez LE, Rengifo E, Lanio ME, Alvarez C, et al. Generation of a murine monoclonal antibody specific for N-glycolylneuraminic acidcontaining gangliosides that also recognizes sulfated glycolipids. *Hybridoma.* 1995;14:551–556.

51. Vazquez AM, Perez A, Hernandez AM, Macias A, Alfonso M, Bombino G, Perez R. Syngeneic anti-idiotypic monoclonal antibodies to an antiNeuGc-containing ganglioside monoclonal antibody. *Hybridoma.* 1998; 17:527–534.
52. López-Requena A, Mateo de Acosta C, Pérez A, Valle A, Lombardero J, Sosa K, Pérez R, Vázquez AM. Chimeric anti-N-glycolyl-ganglioside and its anti-idiotypic MAbs: immunodominance of their variable regions. *Hybrid Hybridomics.* 2003;22:235–243.
53. López-Requena A, De Acosta CM, Moreno E, González M, Puchades Y, Talavera A, Vispo NS, Vázquez AM, Pérez R. Gangliosides, Ab1 and Ab2 antibodies I: towards a molecular dissection of an idiotype-antiidiotype system. *Mol Immunol.* 2007;44:423– 433.
54. Fernandez-Marrero Y, Hernandez T, Roque-Navarro L, Talavera A, Moreno E, Grinan T, Vazquez AM, de Acosta CM, Perez R, López-Requena A. Switching on cytotoxicity by a single mutation at the heavy chain variable region of an anti-ganglioside antibody. *Mol Immunol.* 2011;48:1059 –1067.
55. Mateo C, Moreno E, Amour K, Lombardero J, Harris W, Perez R. Humanization of a mouse monoclonal antibody that blocks the epidermal growth factor receptor: recovery of antagonistic activity. *Immunotechnology*. 1997; 3:71-81.
56. Perez A, Lombardero J, Mateo C, Mustelier G, Alfonso M, Vazquez AM and Perez R. Immunogenetic analysis of variable regions encoding AB1 and gamma-type AB2 antibodies from the NeuGc-containing ganglioside family. *Hybridoma.* 2001 Aug;20(4):211-21.
57. Martínez D, Pupo A, Cabrera L, Raymond J, Holodick NE and Hernández AM. B-CD8+ T Cell Interactions in the Anti-Idiotypic Response against a Self-Antibody. *J. Immuno. Res.* Volume 2017, Article ID 2860867.
58. Kohler H, Pashov A, Kieber-Emmons T. The Promise of Anti-idiotype Revisited. *Front Immunol.* 2019 Apr 12;10:808.
59. Iozzo RV, Schaefer L. Proteoglycan form and function: A comprehensive nomenclature of proteoglycans. *Matrix Biol.* 2015 Mar;42:11-55.
60. Theocharis AD, Tsolakis I, Tzanakakis GN, Karamanos NK. Chondroitin sulfate as a key molecule in the development of atherosclerosis and cancer progression. *Adv Pharmacol*. 2006;53:281-95.

TABLES

Table I. Fasting levels of biochemical and clinical parameters in cholesterol-fed IR rats treated with chP3R99 mAb

Parameter	Acute mAb Injections (4.5 mg/kg, IV)		Immunizations (200 µg, SC, 6 weeks)	
	hR3 mAb (n=3)	chP3R99 mAb (n=3)	hR3 mAb (n=5)	chP3R99 mAb (n=6)
Glucose (mmol/L)	7.9 ± 0.5	8.0 ± 0.8	11.5 ± 1.5	9.6 ± 0.9
Insulin (pmol/L)	1058.0 ± 170.3	1270.0 ± 189.4	1260 ± 195.0	1267 ±134.6
HOMA-IR (AU)	147.5 ± 21.3	169.1 ± 8.3	69.6 ± 8.1	73.3 ± 7.6
Leptin (µg/mL)	56.9 ± 11.2	65.7 ± 13.5	119.7 ± 13.4	101.5 ± 15.1
LDL (mmol/L)	2.0 ± 0.2	1.6 ± 0.1	1.8 ± 0.1	2.8 ± 0.1
Total Chol (mmol/L)	5.4 ± 0.4	4.6 ± 0.2	7.4 ± 0.4	7.1 ± 0.3
TG (mmol/L)	3.7 ± 0.5	4.9 ± 0.4	2.0 ± 0.2	1.9 ± 0.2
AST (µg/mL)	20.8 ± 1.5	20.2 ± 0.4	20.7 ± 0.9	19.6 ± 2.1
ALT (µg/mL)	6.0 ± 0.9	6.2 ± 1.4	7.1 ± 1.0	5.1 ± 2.2
Haptoglobin (mg/L)	11.3 ± 2.7	3.4 ± 1.6	10.6 ± 3.1	9.6 ± 1.9
CRP (mg/L)	231.7 ± 44.8	300.2 ± 31.9	311.9 ± 55.4	350.3 ± 37.7
β2-Microglobuline (µg/mL)	7.8 ± 2.4	7.6 ± 2.0	8.0 ± 1.2	9.5 ± 1.3

Results are mean±SEM. Two-tailed Mann-Whitney *U* test or unpaired Student *t* test compared with control groups.

Table II. Cytokine and growth factors levels in plasma from cholesterol-fed IR rats treated with chP3R99 mAb.

Parameter	10-wk-old rats on chow		Acute mAb injections in IR rats (4.5 mg/kg, IV)		Immunizations in IR rats (200 µg, Sc, 6 weeks)	
	Control rats (n=5)	IR rats (n=5)	hR3 mAb (n=3)	R99 mAb (n=3)	hR3 mAb (n=5)	R99 mAb (n=6)
G-CSF (pg/mL)	112.4±17.1	230.1±30.6**	238.1±34.8	168.2±19.5	200.4±37.0	132.8±32.1
GM-CSF (pg/mL)	130.4±12.9	306.5±169.3	426.1±286.1	351±112.2	646.4±148.6	543.0±239.6
Eotaxin (pg/mL)	13.5±2.5	18.6±2.1	20.1±1.3	12.2±1.9	25.6±4.5	39.7±7.6
MIP-1a (pg/mL)	21.9±1.6	32.4±4.4	23.9±9.5	18.9±3.5	24.7±6.6	38.4±7.8
MIP-2 (pg/mL)	309.7±11.8	357.0±35.3	405.4±61.4	311.2±34.6	439.3±52.2	465.0±62.8
MCP-1 (µg/mL)	1.2±0.1	1.5±0.2	2.1±0.7	1.1±0.3	2.4±0.6	2.3±0.7
Fractalkine (pg/mL)	84.7±2.2	114.3±14.6	81.4±18.3	80.9±26.9	73.6±15.6	147.4±50.5
RANTES (pg/mL)	1.9±0.3	3.2±0.4*	0.3±0.0	0.3±0.0	1.1±0.5	1.6±0.4
LIX (µg/mL)	3.7±0.7	4.8±0.9	0.6±0.1	0.5±0.1	3.8±0.8	2.7±1.1
IP-10 (pg/mL)	594.1±17.5	663.3±91.3	475.4±67.4	431.4±56.6	516.3±80.7	511.3±49.3
EGF (pg/mL)	10.9±5.4	8.4±2.8	4.3±4.1	ND	19.1±12.9	22.4±13.2
GRO/KC (pg/mL)	503.4±129.4	721.1±113.7	556.3±247.3	214±25.2	566±198.5	809.2±196.1
VEGF (pg/mL)	33.8±15.6	95.6±32.6	136.7±54.2	54.9±45.4	64.6±35.6	126.9±77.2
TGF-β1 (µg/mL)	27.4±12.5	40.9±10.5	1.8±1.6	1.2±0.6	34.7±1.1	23.3±12.7
TGF-β2 (µg/mL)	1.4±0.6	1.8±0.4	0.2±0.0	0.1±0.0	1632.0±573.8	877.9±454.7
INF-γ (pg/mL)	343.8±248.0	1097.0±189.4*	778.4±638.1	ND	ND	ND
TNF-α (pg/mL)	16.5±2.5	32.5±7.2*	87.1±53.5	7.8±4.1	49.2±12.8	61.7±23.9
IL-1α (µg/mL)	198.5±26.9	437.3±115.5	199.5±143.6	54.9±23.6	278.4±84.8	212.1±84.1
IL-1β (pg/mL)	1429.0±461.1	947.2±289.6	2221.0±450.9	977.4±357.8	3800.0±1820.0	2935.0±623.5
IL-2 (pg/mL)	77.4±10.6	161.1±32.1*	204.4±112.7	152.4 ± 90.9	250.8±83.6	262.0±35.4
IL-5 (pg/mL)	99.8±2.9	123.9±11.4	179.4±74.5	90.8±10.8	162.9±22.9	236.3±46.5
IL-6 (µg/mL)	34.7±2.6	153.1±13.9****	147.5±21.3	169.1±8.3	119.7±13.5	101.5±15.1
IL-10 (pg/mL)	1242.0±422.9	839.9±242.2	2084.0±487.9	913.3±332.7	3304.0±1567.0	2555.0±497.0
IL-12p70 (pg/mL)	222.5±48.3	531.2±172.0	1648.0±1037.0	176.9±39.6	668.7±178.3	627.1±183.1
IL-13 (pg/mL)	17.4±5.8	29.9±13.2	104.1±72.4	1.46±1.0	64.4±15.1	59.9±21.9
IL-17A (pg/mL)	25.5±7.9	42.9±17.4	110.6±70.3	15.9±4.6	62.4±20.9	44.6±14.5
IL-18 (pg/mL)	292.9±71.7	518.3±140.9	295.7±85.1	325.9±144.1	271.8±83.9	608.2±330.2

Figure 1

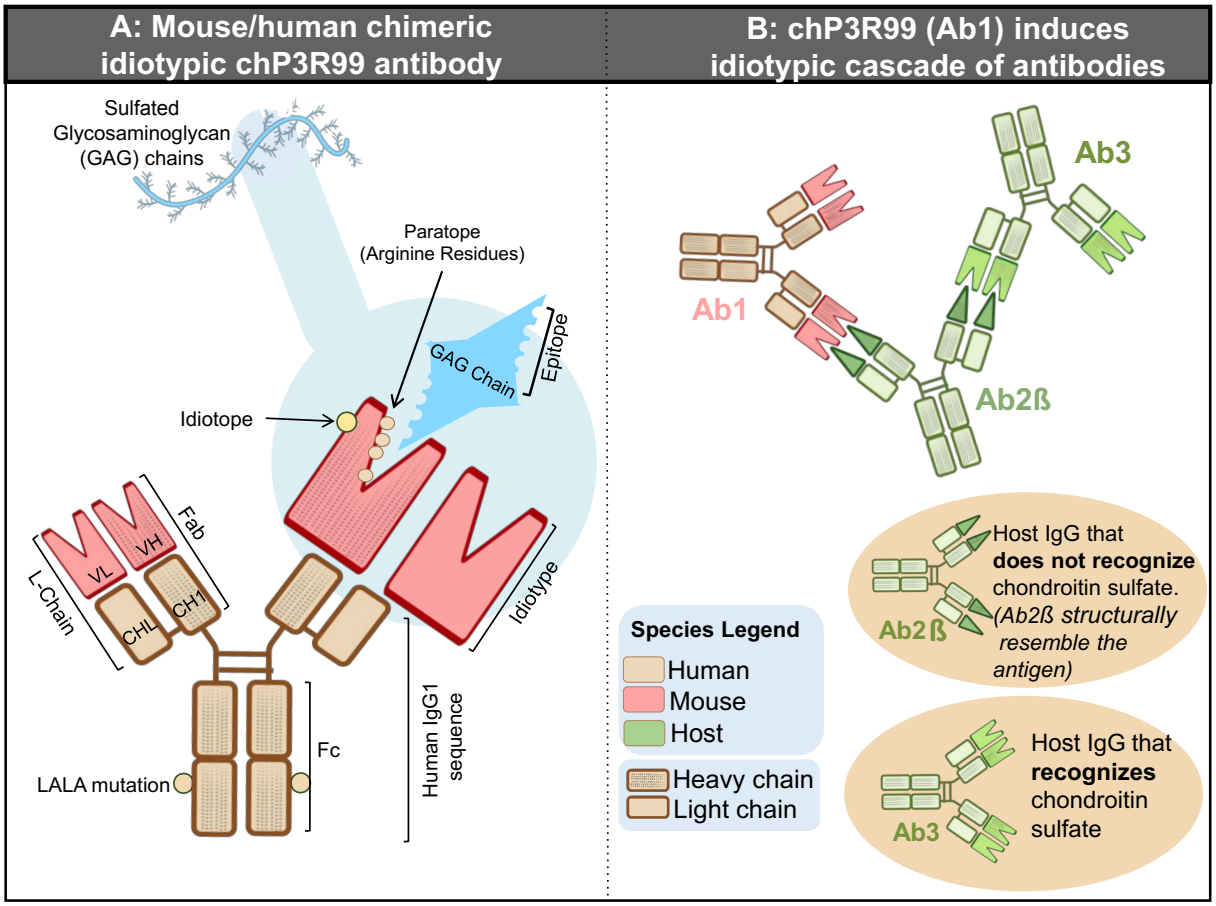

Figure 1: Summary of the main features of chP3R99 mAb. (A) Chimeric mAb composed by mouse variable regions (idiotype) and human IgG1constant regions mutated to abrogate the binding to Fcγ receptors and the complement system activation (LALA mutation). The antigen recognition site of chP3R99 is enriched in arginine residues involved in the 'Acute'(competitive) interaction with the lipoprotein binding site on glycosaminoglycan side chains of proteoglycans. The variable regions of chP3R99 contains immunogenic epitopes (idiotopes) including the antigen-combination site (paratopes). (B) Schematic of the putative idiotypic cascade mounted by chP3R99 mAb (Ab1) to produce anti-idiotypic antibodies (Ab2, 2nd generation of Abs) and anti-anti-idiotypic antibodies (Ab3, 3rd generation of Abs) mAb by the host.

Figure 2

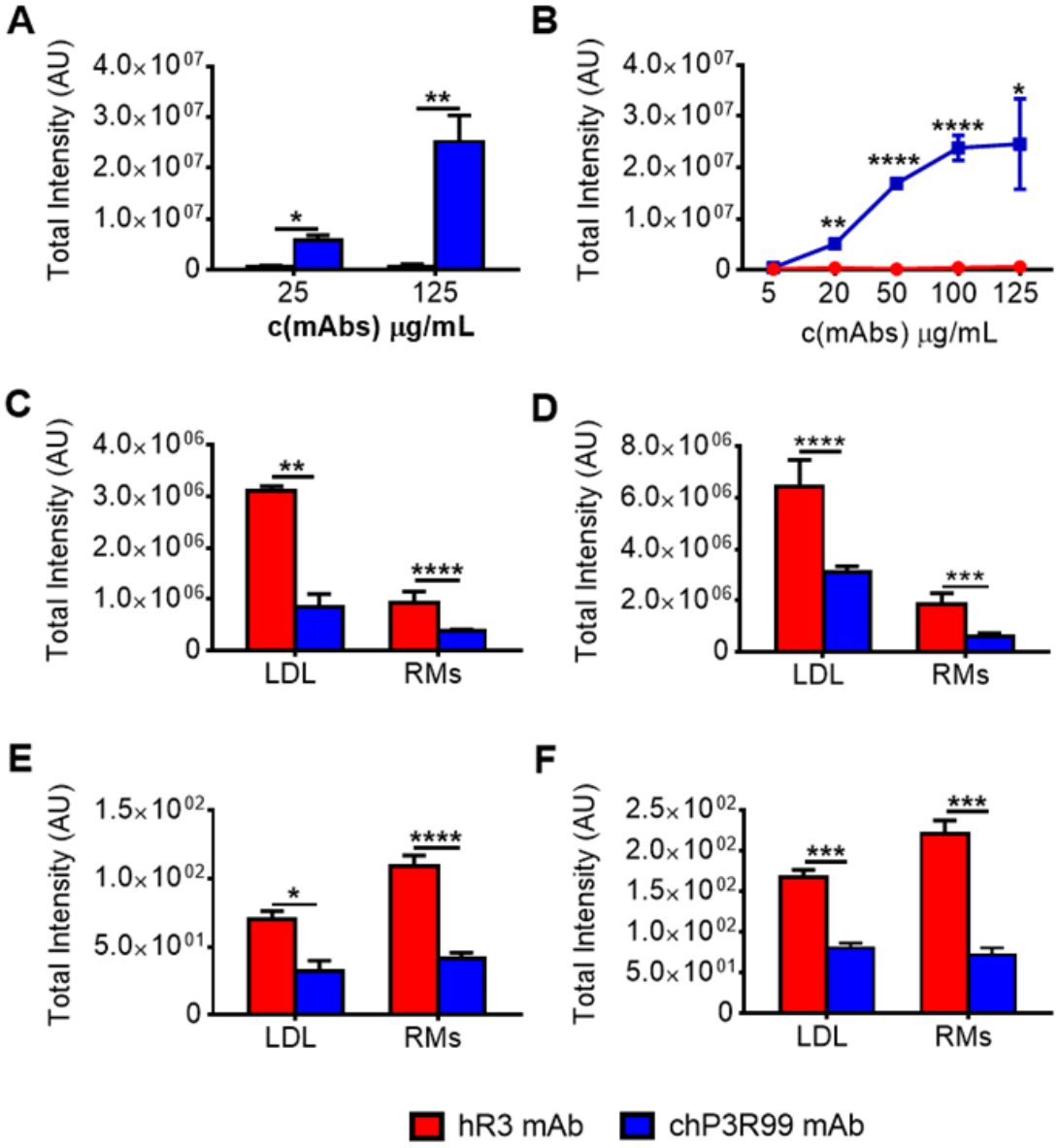

Figure 2. chP3R99 mAb blocking properties *in vitro*. Recognition of chP3R99 mAb to (A) Chondroitin sulfate (CS) and (B) Extracellular matrix (ECM) derived from vascular smooth muscle cells (VSMC) from rat aorta explants. Amino-reactive 3D chambered slides (Nexterion H) coated with CS (1 mg/mL) were incubated with chP3R99 mAb or the isotype-matched control (25 or 125 µg/mL) whereas ECM-coated Lab Tek II chambers were incubated with increasing concentrations of the mAbs (0-125 µg/mL). Recognition was detected with a Cy3-conjugated goat anti-human IgG serum. Inhibitory effect of chP3R99 mAb on lipoprotein binding to (A) CS and (B) ECM *in vitro*. Wells were pre-incubated for 90 min with the mAbs (250 µg/mL) followed by incubation with the lipoproteins (Cy3-LDL or Cy5-RM) at 250 µg/mL. Slides were scanned at 520 nm and/or 640 nm to determine the fluorescence associated with specific binding (GenePix 4000B). Cholesterol associated with bound lipoproteins to CS (E) and the ECM (F) was estimated based on the total intensity and the concentration of cholesterol per particle of lipoprotein/intensity AU. Specificity was assessed using hR3 mAb as isotype-matched control. Results are expressed as the mean±SEM of at least three experiments. Mann-Whitney *U* test, *$p<0.05$, **$p<0.01$, ****$p<0.0001$. RMs: remnants.

Figure 3

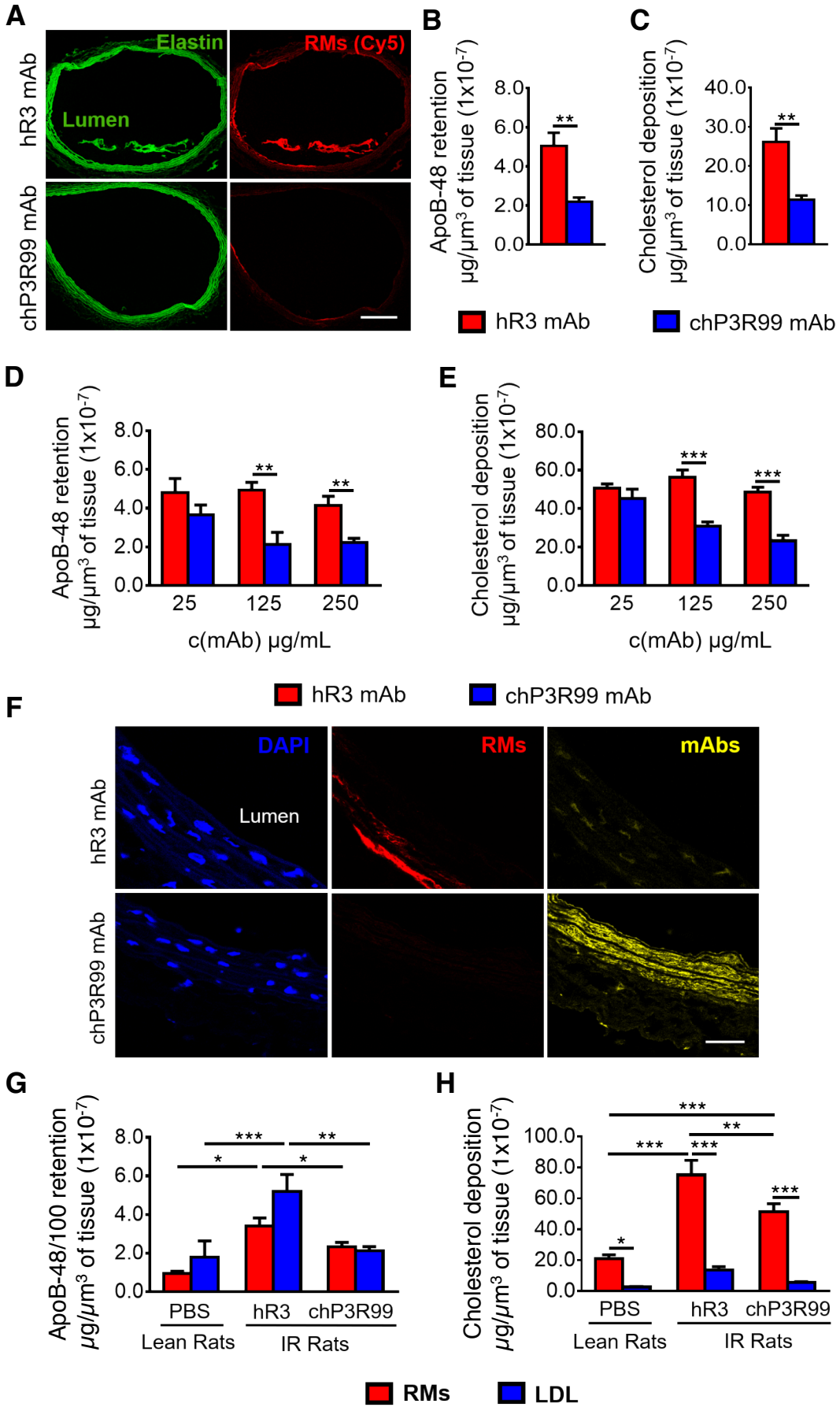
A
Elastin
RMs (Cy5)
Lumen
hR3 mAb
chP3R99 mAb
B
ApoB-48 retention
µg/µm³ of tissue (1x10⁻⁷)
8.0
6.0
4.0
2.0
0.0
**
C
Cholesterol deposition
µg/µm³ of tissue (1x10⁻⁷)
40.0
30.0
20.0
10.0
0.0
**
hR3 mAb
chP3R99 mAb
D
ApoB-48 retention
µg/µm³ of tissue (1x10⁻⁷)
8.0
6.0
4.0
2.0
0.0
**
**
25
125
250
c(mAb) µg/mL
E
Cholesterol deposition
µg/µm³ of tissue (1x10⁻⁷)
80.0
60.0
40.0
20.0
0.0
***
***
25
125
250
c(mAb) µg/mL
hR3 mAb
chP3R99 mAb
F
DAPI
RMs
mAbs
Lumen
hR3 mAb
chP3R99 mAb
G
ApoB-48/100 retention
µg/µm³ of tissue (1x10⁻⁷)
8.0
6.0
4.0
2.0
0.0
***
**
*
*
PBS
hR3
chP3R99
Lean Rats
IR Rats
H
Cholesterol deposition
µg/µm³ of tissue (1x10⁻⁷)
100.0
80.0
60.0
40.0
20.0
0.0
***
**
***
***
*
***
PBS
hR3
chP3R99
Lean Rats
IR Rats
RMs
LDL

Figure 3. Acute effect of chP3R99 mAb on arterial retention of chylomicron remnants in insulin-resistant (JCR:LA-cp) rats.

Carotid arteries from 12-week-old IR rats (n=4-6 per condition) were pre-perfused *ex vivo* with chP3R99 mAb for 20 min followed by the perfusion of fluorescently labeled lipoproteins.

(A) Representative confocal images showing the blockade of Cy5-RM (red) arterial retention (90 µg/mL) by the chP3R99 mAb (125 µg/mL) Morphology in green. Magnification 20X, Scale bar=100 µm.

(B) Quantification of RM particle number expressed as ApoB-48 molecules per volume unit.

(C) Cholesterol deposition in carotids per volume unit.

(D) Dose-response effect of chP3R99 on Cy5-RM (150 µg/mL) arterial retention and

(E) on cholesterol deposition in IR rats. (F) Representative images showing a reduction of Cy5-RM retention (red) associated with the arterial accumulation of chP3R99 mAb perfused at 250 µg/mL (yellow). Counterstaining of nuclei in blue (DAPI). Magnification 100X, Scale bar=50 µm.

(G) Relative inhibitory effect of chP3R99 on Cy5-RM retention in the presence of equivalent concentrations of Cy3-LDL and

(H) on cholesterol deposition. Total fluorescent intensity at 532 nm (LDL) and 635 nm (RM) was determined and the corresponding number of ApoB-48/100 particles was estimated relative to the total intensity associated with a known concentration of ApoB in the perfusate *$p<0.05$. Cholesterol content in the vessels was estimated as per ApoB, relative to the total intensity associated with cholesterol content in the perfusate. Lean rats were perfused solely with lipoprotein preparation as control whereas specificity was assessed by using the hR3 mAb as isotype-matched control.

Data are mean±SEM. n=5 sections/animal, 10 Z-sections/slice. *$p<0.05$, one-way Anova and Bonferroni.

Figure 4

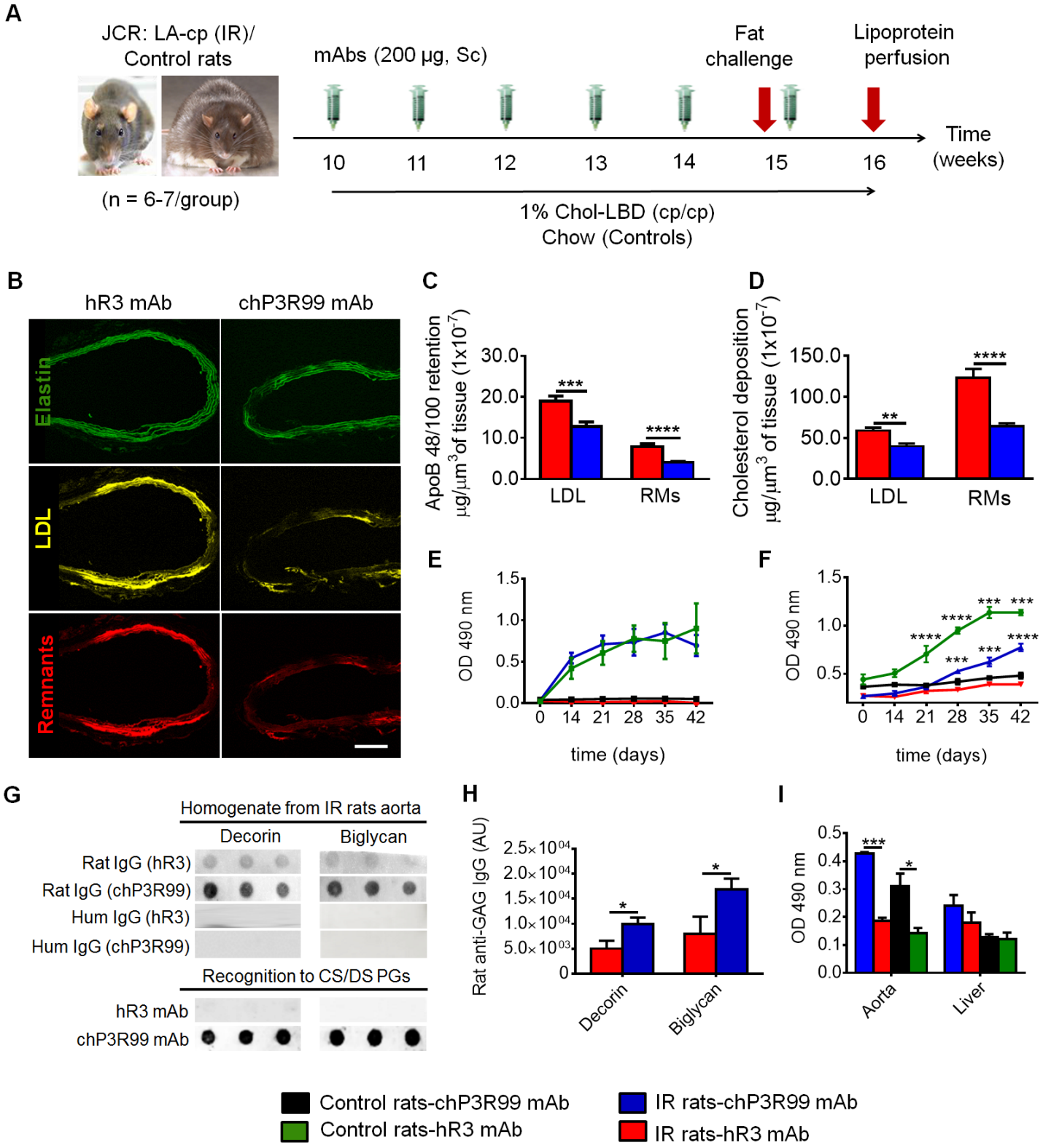
A
JCR: LA-cp (IR)/
Control rats
(n = 6-7/group)
mAbs (200 µg, Sc)
Fat
challenge
Lipoprotein
perfusion
10
11
12
13
14
15
16
Time
(weeks)
1% Chol-LBD (cp/cp)
Chow (Controls)
B
hR3 mAb
chP3R99 mAb
Elastin
LDL
Remnants
C
ApoB 48/100 retention
µg/µm3 of tissue (1x10-7)
30.0
20.0
10.0
0.0
***
****
LDL
RMs
D
Cholesterol deposition
µg/µm3 of tissue (1x10-7)
150.0
100.0
50.0
0.0
**
****
LDL
RMs
E
OD 490 nm
1.5
1.0
0.5
0.0
0
14
21
28
35
42
time (days)
F
OD 490 nm
1.5
1.0
0.5
***
***
****
****
***
***
****
0
14
21
28
35
42
time (days)
G
Homogenate from IR rats aorta
Decorin
Biglycan
Rat IgG (hR3)
Rat IgG (chP3R99)
Hum IgG (hR3)
Hum IgG (chP3R99)
Recognition to CS/DS PGs
hR3 mAb
chP3R99 mAb
H
Rat anti-GAG IgG (AU)
2.5×10^04
2.0×10^04
1.5×10^04
1.0×10^04
5.0×10^03
0
*
*
Decorin
Biglycan
I
OD 490 nm
0.5
0.4
0.3
0.2
0.1
0.0
***
*
Aorta
Liver
Control rats-chP3R99 mAb
Control rats-hR3 mAb
IR rats-chP3R99 mAb
IR rats-hR3 mAb

Figure 4. Effect of the vaccination with chP3R99 mAb on arterial lipoprotein retention in insulin-resistant (IR) rats (JCR:LA-cp).

(A) Study Design: Both IR and control rats received six subcutaneous injections of chP3R99 mAb or the isotype-matched control hR3 (200 µg/week). Vaccinated IR rats underwent an *ex vivo* carotid perfusion of equivalent amounts of Cy3-LDL and Cy5-RM lipoproteins (150 µg/mL).

(B) Representative images of the arterial retention of RM (red) and LDL (yellow) in IR rats. Morphology in green. Magnification 20X, Scale bar=100 µm.

(C) Quantification of lipoprotein retention in the vessels (n=5 sections/animal, 10-Z sections/slice). The corresponding number of ApoB-48/100 particles was estimated relative to the total intensity associated with a known concentration of ApoB in the perfusate, $*p<0.05$.

(D) Arterial cholesterol deposition relative to the total intensity associated with a known concentration of cholesterol in the perfusate, $*p<0.05$.

(E) Kinetics of induction of anti-idiotypic Abs (Ab2) in rats immunized with chP3R99 mAb. The Ab2 response was assessed by subtracting the reactivity of the sera to the isotype-match control (anti-isotypic response) from the total response directed to chP3R99 by ELISA.

(F) Kinetics of induction of anti-CS Abs in rats (Ab3 response).

(G) Detection of Ab3 within the aorta by Dot Blot. Membranes were spotted with CS-PGs (20 µg/dot) and incubated with aorta homogenates (1 mg/mL) from immunized rats.

(H) Relative quantification of anti-CS Abs in aorta homogenates.

(I) Accumulation of anti-CS Abs in tissue lysates by ELISA. GAG-coated plates (10 µg/mL) were incubated with rat sera (1/200) or the tissue lysates (1 mg/mL). The presence of rat IgG in the tissues was detected by an anti-rat IgG secondary serum whereas the recognition of P3R99 to proteoglycans or its presence in the aorta homogenates were assessed utilizing an anti-human IgG secondary serum conjugated to HRP. Data are mean±SEM, $*p<0.05$, one-way Anova and Bonferroni.

Figure 5

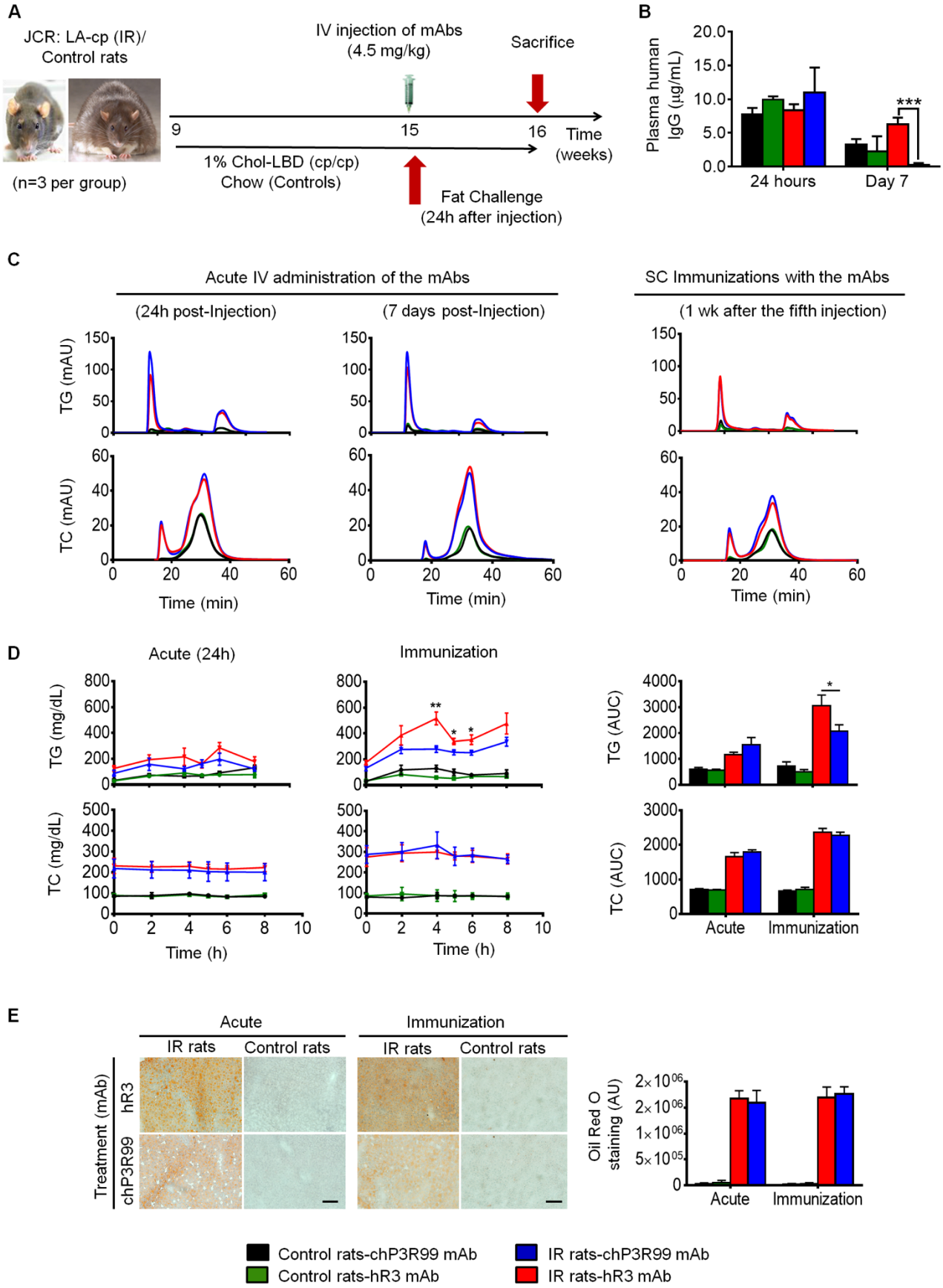
A
JCR: LA-cp (IR)/
Control rats
(n=3 per group)
IV injection of mAbs
(4.5 mg/kg)
Sacrifice
9
15
16
Time
(weeks)
1% Chol-LBD (cp/cp)
Chow (Controls)
Fat Challenge
(24h after injection)
B
Plasma human IgG (μg/mL)
20.0
15.0
10.0
5.0
0.0
***
24 hours
Day 7
C
Acute IV administration of the mAbs
(24h post-Injection)
(7 days post-Injection)
SC Immunizations with the mAbs
(1 wk after the fifth injection)
TG (mAU)
TC (mAU)
Time (min)
D
Acute (24h)
Immunization
TG (mg/dL)
TC (mg/dL)
Time (h)
TG (AUC)
TC (AUC)
Acute
Immunization
E
Acute
Immunization
IR rats
Control rats
Treatment (mAb)
hR3
chP3R99
Oil Red O staining (AU)
Control rats-chP3R99 mAb
Control rats-hR3 mAb
IR rats-chP3R99 mAb
IR rats-hR3 mAb

Figure 5. Effect of acute administration of chP3R99 mAb and the immunization in lipoprotein metabolisms.

(A) Acute intravenous administration of chP3R99 mAb in lean control and cholesterol-fed IR rats (n=3). The rats were inoculated with 4.5 mg/kg (body weight) of chP3R99 mAb in PBS through the jugular vein at 15 weeks of age.

(B) Quantification of human IgG in rat sera 24 hours and seven days after bolus administration of the mAbs.

(C) Triglyceride and cholesterol FPLC fractions in pooled plasma from rats subjected to intravenous inoculation of or immunization with chP3R99 mAb.

(D) Postprandial study in rats. At 15 weeks of age, the rats were fasted overnight and subjected to an oral fat challenge.

(E) Neutral lipids content in the liver of rats visualized by ORO staining. Scale bar=100μm; Magnification 20X. Five images were quantified per animal. Specificity was assessed using hR3 mAb as isotype-matched control. Results are expressed as mean±SEM. Student *t*-test, $*p<0.05$.